




# Transcrystallization of the acetylated bamboo fiber/polypropylene composite under isothermal crystallization

Yu-Shan Jhu<sup>1</sup> · Ke-Chang Hung<sup>1</sup> · Jin-Wei Xu<sup>1</sup> · Tung-Lin Wu<sup>2,3</sup> ·  
Jyh-Horng Wu<sup>1</sup> 

Received: 8 July 2020 / Accepted: 25 February 2021 / Published online: 25 March 2021

© The Author(s), under exclusive licence to Springer-Verlag GmbH Germany, part of Springer Nature 2021

## Abstract

The crystallization behaviors of acetylated bamboo fiber (BF)/polypropylene (PP) composites were assessed using differential scanning calorimetry (DSC) through isothermal crystallization. The transcrystalline (TC) morphologies of composites were observed through polarized optical microscopy (POM), and their surface free energies were calculated based on Hoffman–Lauritzen theory. Isothermal DSC thermograms demonstrated that acetylated BF with higher weight percentage gains (WPGs, ~19%) exhibited a decreased crystallization rate of the PP matrix. POM images indicated that BF as a nucleation agent induced the TC layer on fiber–PP matrix interfaces. However, when WPG reached 19%, the TC layer was not observed on the BF surface and crystal growth was principally observed in the PP matrix bulk. Based on Hoffman–Lauritzen theory, the folding-surface free energy ( $\sigma_e$ ) and the work of chain folding ( $q$ ) for acetylated BF/PP composites were estimated to be higher than those for PP composites with unmodified BF. These results indicate that BFs with different WPGs could affect the crystallization behavior of the PP matrix by inducing or hindering TC on BF–PP matrix interfaces.

---

Yu-Shan Jhu and Ke-Chang Hung contributed equally to this work.

---

✉ Jyh-Horng Wu  
eric@nchu.edu.tw

<sup>1</sup> Department of Forestry, National Chung Hsing University, Taichung 402, Taiwan

<sup>2</sup> College of Technology and Master of Science in Computer Science, University of North America, Chantilly, VA 22033, USA

<sup>3</sup> Department of Wood Science and Design, National Pingtung University of Science and Technology, Pingtung 912, Taiwan

## Introduction

Bamboo has a faster growth rate compared with other plants and grows abundantly across Asia and South America (Scurlock et al. 2000; Liu et al. 2014; Mori et al. 2019). Furthermore, bamboo possesses high flexibility and highly specific mechanical properties because of the longitudinal alignment of fibers that include approximately 60% cellulose with a high content of lignin and a relatively small microfibril angle (Li et al. 2015; Liu et al. 2015, 2016). Because of these properties, bamboo has been employed in various fields, such as furniture, handicrafts, and flooring. The valuable properties of bamboo fibers (BFs) have long been recognized, and they are thus used as efficient reinforcement in polymer composites (Chen et al. 1998; Ismail et al. 2002; Okubo et al. 2004; Chattopadhyay et al. 2011; Wang et al. 2014; Cheng et al. 2015; Yang et al. 2015). Therefore, BF is considered a valuable natural fiber and can have potential applications in the polymer composite industry. However, hygroscopicity and incompatibility between the hydrophilic lignocellulosic and hydrophobic thermoplastic have been identified as major limitations to the application of bamboo–plastic composites. Several studies have attempted to overcome these limitations by modifying lignocellulosic materials by using physical and chemical approaches, such as heat treatment, esterification, alkaline treatment, steam explosion treatment, and coupling agent addition, to reduce their hygroscopicity and increase their dimensional and thermal stabilities (Rowell 1983; Deshpande et al. 2000; Keener et al. 2004; Okubo et al. 2004; Das and Chakraborty 2008; Hung and Wu 2010). The acetylation of lignocellulosic fibers is one of the principal chemical approaches and has received considerable attention. Numerous studies have reported an improvement in compatibility at fiber–polymer interfaces by using this chemical approach (Lisperguer et al. 2007; Hung et al. 2012, 2016). However, the resulting microstructure of the polymer matrix, especially as reflected by crystallization and crystal state, has a significant effect on the quality and properties of end products, because it is dependent on the thermal and press history during the manufacturing process (Kamal and Chu 1983).

In semicrystalline polymer composites, natural fibers may act as heterogeneous nucleating agents and orientation templates for polymer crystallization. When the melted polymer matrix becomes cold, nucleation crystallization occurs along the fiber–matrix interface with massive nuclei. Subsequently, the crystal grows unidirectionally along the fiber axis until the front is impeded by the growth of spherulites, which is nucleated in the polymer matrix. Therefore, an oriented crystalline layer, known as a transcrystalline (TC) layer, develops at the fiber–matrix interface. Researchers have reported that the development of the TC layer was observed in numerous polymer systems with fibrous fillers and that this crystalline structure was affected by several different factors, such as the filler type, the surface topography of the filler, thermal history, crystallization temperature, and surface energy of constituents (Thomason and Van Rooyen 1992; Cai et al. 1997; Wang and Liu 1999; Quan et al. 2005; Borysiak 2013). Furthermore, the TC layer has been proposed to improve the interfacial compatibility and enhance the

load-transfer efficiency between the polymer matrix and the fiber, thereby improving the mechanical properties of composites (Han et al. 2014; Gao et al. 2015). To the authors' knowledge, little information is available regarding the effect of acetylated bamboo fibers on the isothermal crystallization behavior of BF/polymer composites. Therefore, the present study investigated certain aspects of the isothermal crystallization kinetics of polypropylene (PP) composites with different weight percent gains (WPGs) of acetylated BFs under isothermal conditions by performing differential scanning calorimetry (DSC) analysis. Furthermore, the primary objective of the present study was to determine the effect of acetylated BFs on transcrystallization in the PP matrix through polarized optical microscopy (POM). The folding-surface free energy ( $\sigma_e$ ) and the work of chain folding ( $q$ ) were examined using Hoffman–Lauritzen theory to investigate the crystal growth rate and the nucleation mechanism of the PP matrix.

## Experimental

### Materials

The 3-year-old kei-chiku bamboo (*Phyllostachys makinoi* Hayata) was generously provided by a local bamboo-processing factory. BFs were extracted from shavings by using hammer milling and sieving to obtain fibers between 24 and 30 mesh (700–550  $\mu\text{m}$ ). All BFs were extracted in a Soxhlet apparatus for 24 h with acetone and washed with distilled water before drying at 75  $^{\circ}\text{C}$  for 24 h. PP pellets, which have a density of 915  $\text{kg}/\text{m}^3$ , a melt flow index of 4–8 g/10 min, and a melting point of 145  $^{\circ}\text{C}$ , were purchased from Yung Chia Chemical Industries Co., Ltd. (Taipei, Taiwan). The particle size of plastic pellets was ground in an attrition mill to less than 100 mesh ( $< 150 \mu\text{m}$ ). Acetone, dimethylformamide (DMF), and acetic anhydride (AA) were purchased from Sigma-Aldrich Chemical Co. (St. Louis, MO, USA).

### Sample preparation

The liquid-phase reaction method was used to acetylate BFs with AA. The concentration ratios of AA:DMF were 0.2:20, 0.3:20, 1:20, and 4:20 (mL/mL) per gram of oven-dried BFs. Acetylated BFs with different degrees of modification were obtained using reaction conditions at 140  $^{\circ}\text{C}$  for 2 h, followed by washing with distilled water for 4 h and drying at 105  $^{\circ}\text{C}$  for 12 h. The WPG of acetylated BFs was calculated using Eq. 1:

$$\text{WPG (\%)} = [(W_1 - W_0)/W_0] \times 100 \quad (1)$$

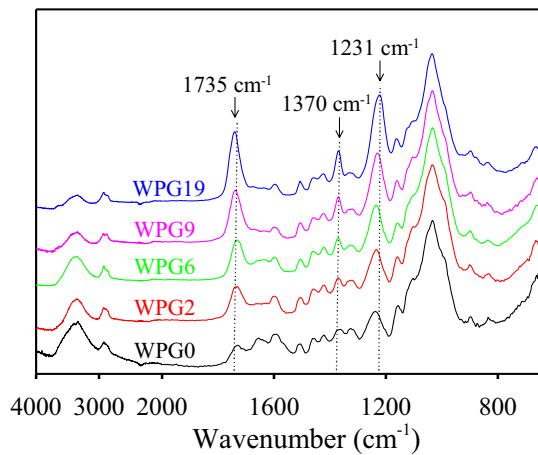
where  $W_0$  and  $W_1$  are the oven-dried weights of BFs before and after acetylation. The resulting WPGs of acetylated BFs were approximately 2%, 6%, 9%, and 19%, designated as WPG2, WPG6, WPG9, and WPG19, respectively. Table 1 summarizes sample codes and reaction conditions for unmodified and various WPGs of

**Table 1** Sample code and reaction conditions for different degrees of acetylated bamboo fibers (BFs)

| BFs    | BF:AA:DMF<br>(g:mL:mL) | Reaction time<br>(min) | WPG of acetylated BF (%)* |
|--------|------------------------|------------------------|---------------------------|
| WPG0** | —                      | —                      | —                         |
| WPG2   | 1:0.2:20               | 120                    | 2.3 ± 0.9                 |
| WPG6   | 1:0.3:20               | 120                    | 5.9 ± 1.1                 |
| WPG9   | 1:1:20                 | 120                    | 8.7 ± 1.6                 |
| WPG19  | 1:4:20                 | 120                    | 19.0 ± 1.5                |

\*Values are the mean ± SD ( $n=5$ )

\*\*WPG0 refers to the unmodified bamboo fibers

**Fig. 1** ATR-FTIR spectra of acetylated bamboo fibers with various WPGs

acetylated BFs. The successful acetylation of these BFs has been confirmed by Fourier transform infrared spectroscopy (FTIR). As shown in Fig. 1, the specific absorption bands of acetyl group at wavenumber 1735, 1370, and 1231  $\text{cm}^{-1}$  increased with increasing WPG of acetylated BFs.

### ATR-FTIR spectral measurement

Attenuated total reflectance Fourier transform infrared (ATR-FTIR) spectra of all unmodified and various WPGs of acetylated BFs were recorded on a Spectrum 100 FTIR spectrometer (PerkinElmer, Buckinghamshire, UK) equipped with a deuterated triglycine sulfate (DTGS) detector and a MIRacle ATR accessory (Pike Technologies, Madison, WI, USA). The spectra were collected by co-adding 32 scans at a resolution of 4  $\text{cm}^{-1}$  in the range from 650 to 4000  $\text{cm}^{-1}$ .

### DSC measurement

DSC measurements were taken using a weight ratio of acetylated BFs to PP powder of 50:50. A total of 3–5 mg of each sample was prepared in DSC aluminum

pans with lids. Isothermal crystallization studies were conducted in a PerkinElmer DSC8000/8500 differential scanning calorimeter (Waltham, MA, USA). All measurements were realized in nitrogen at a flow rate of 20 mL/min. First, each sample was preliminarily heated from 20 to 190 °C at a heating rate of 100 °C/min. The temperature was then held for 3 min to eliminate the thermal and mechanical history and ensure a nucleus-free melt. Second, the samples were rapidly cooled at a cooling rate of 600 °C/min to the isothermal crystallization temperature ( $T_c$ ) of 122, 124, 126, 128, and 130 °C. The samples were maintained at the desired isothermal temperature for 15 min until the crystallization process was almost complete. Third, the sample was heated to 190 °C at a heating rate of 20 °C/min.

## POM

POM was performed using an Olympus BX53M optical microscope (Tokyo, Japan) equipped with crossed polarizers. The crystallization process of unmodified and acetylated BF/PP composites was performed by heating the samples for 10 min on a hot stage to the melting point of 190 °C (LNP 95, LINKAM, Surrey, UK) to eliminate residual anisotropy and complete the melting process. The samples were then rapidly cooled to the desired isothermal temperature (122, 124, 126, 128, and 130 °C) at a cooling rate of 50 °C/min. The crystallization morphology of the samples was recorded as photographs by using a digital camera, and these photographs were recorded at a certain interval.

## Results and discussion

### Isothermal DSC thermograms

To investigate the crystalline conversion of BF/PP composites as a function of time at a constant temperature, their isothermal crystallization behavior was visualized. As displayed in Fig. 2, DSC thermograms for the isothermal crystallization of PP with unmodified and acetylated BFs are presented by rapidly cooling a molten polymer matrix to the crystallization temperature ( $T_c$ ) after completely melting it at 190 °C for 3 min. Figure 2 illustrates that crystallization was preceded by a short period where the temperature of the sample approaches  $T_c$ . The heat flow gradually increases to an evident peak, caused by the evolution of the enthalpy of crystallization. After the peak, crystallization exhibited a significant reduction in speed when the heat flow is not noticeably different, indicating that crystallization has been completed. Furthermore, exothermic peaks shifted to a higher period value with increasing  $T_c$  for all the samples, indicating that the crystallization of the PP matrix was affected by  $T_c$ . A study reported (Supaphol and Spruiell 2001) that the evolution rate of crystallization enthalpy was significantly dependent on the kinetics of the crystallization process, which is strongly sensitive to changes in  $T_c$ . However, for samples with a WPG of 2–9%, there were

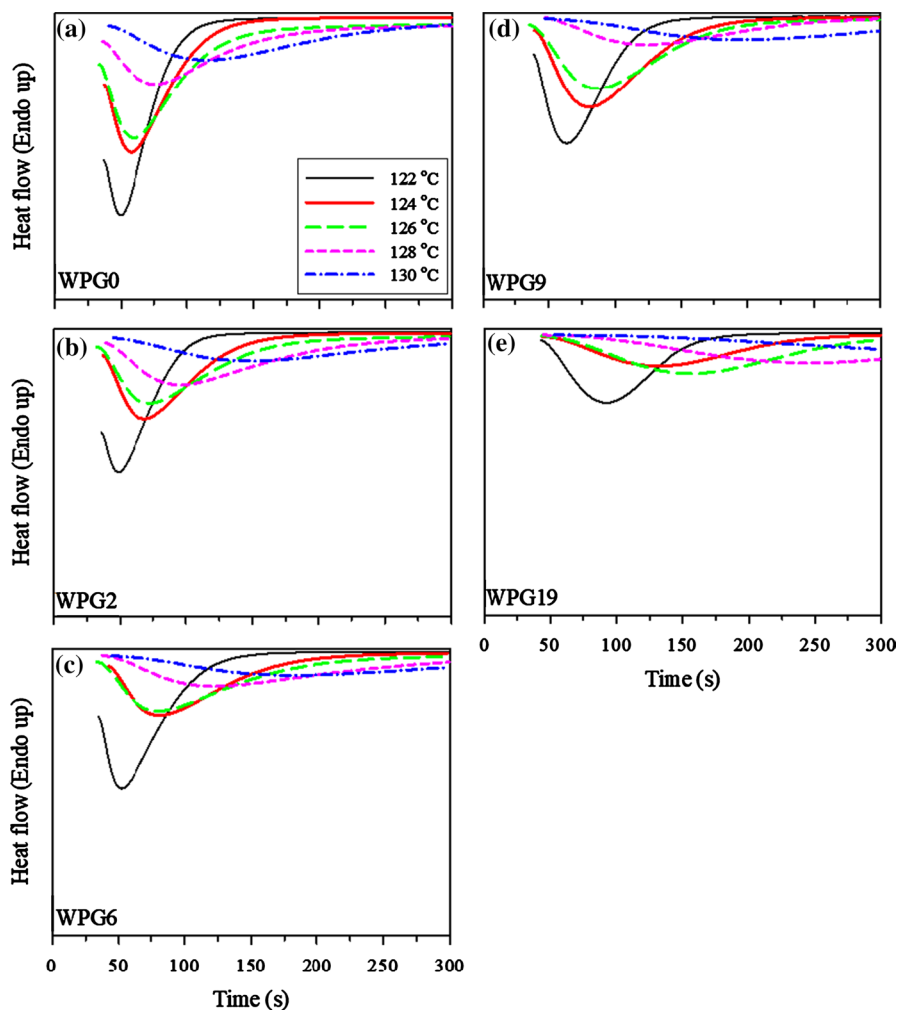


**Fig. 2** Differential scanning calorimetry thermograms of polypropylene with various acetylated bamboo fibers at different isothermal crystallization temperatures. **a** WPG0, **b** WPG2, **c** WPG6, **d** WPG9, and **e** WPG19

no significant differences in the crystallization rate at different  $T_c$ . When WPG reached 19%, the crystallization exothermic peak shifted to a higher temperature. These results indicate that acetylated BFs insignificantly accelerated the crystallization of the PP matrix, whereas acetylated BFs with higher WPG (~19%) reduced the crystallization rate of the PP matrix. A similar result was reported in a previous study (Jhu et al. 2019). It is speculated that the acetylated BFs with higher WPG have more hydrophobic acetyl moieties attached to the fiber surface,

which will cause homogeneous crystal growth of PP matrix, thereby reducing its crystallization rate.

### Observation in the crystallization of BF/PP composite from POM

The crystallization process of a thin PP film with a BF was observed from POM images. Figure 3 compares the spherulitic morphology of all samples in the front of snapshots taken every 50 s during the hot stage when the preset temperature of 130 °C was reached. For WPG0, once the isothermal time reached 50 s, the super-molecular structure, which was identified as the TC layer, was observed. Borysiak (2013) reported that when the molten PP matrix was cooled in contact with wood fiber, the proximity of sites on the fiber–PP interface inhibited the lateral growth of resultant spherulites, resulting in crystallization developing in the normal direction of the wood fiber surface. The appearance of the TC layer indicated that the unmodified BF had a high ability for heterogeneous nucleation. Results indicated that the nucleation of PP spherulites, as well as regular transcrystalline growth, appeared along fiber–matrix interfaces. These observations support that BF accelerates the crystallization of the PP matrix (Phuong and Girbert 2010; Hsu et al. 2018). Furthermore, the micrographs of acetylated BFs with 2–9% WPG, which were embedded in the molten PP matrix, demonstrated that PP crystallization preferentially occurred

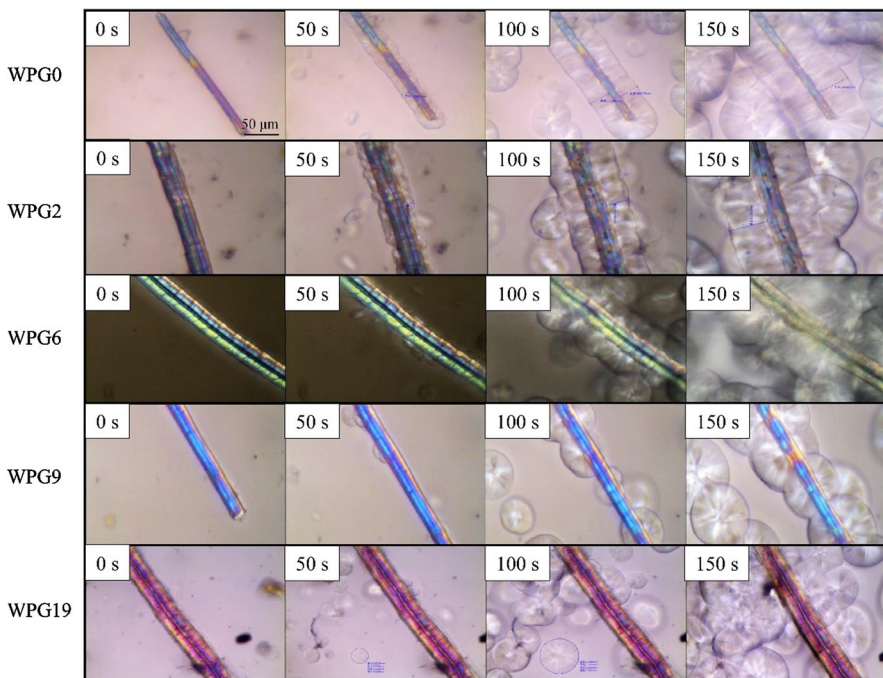


**Fig. 3** POM images of polypropylene with various acetylated bamboo fibers under an isothermal crystallization temperature of 130 °C at different crystallization times

along the BF–PP interface. However, the nucleation density on the surface of those acetylated BFs was significantly lower than the nucleation density of unmodified BF (WPG0). Furthermore, PP reinforced with WPG19 BF displayed different outcomes; the TC layer was not formed on the surface of acetylated BF (WPG19), and main nucleation and crystal growth were observed in the PP matrix bulk. A previous study (Jhu et al. 2019) indicated that this result may be attributed to acetylated BFs with higher WPG causing homogeneous crystal growth as aforementioned. Therefore, the formation and growth of the TC layer are strongly affected by the degree of BF acetylation; BF acetylation with higher WPG does not induce TC on the BF–PP interface. A similar result was reported by Borysiak (2013) who determined that treatment of the lignocellulose surface with various chemicals, such as propionic anhydride and succinic anhydride, inactivates surface features responsible for nucleating the transcrystallinity of lignocellulose/PP composites.

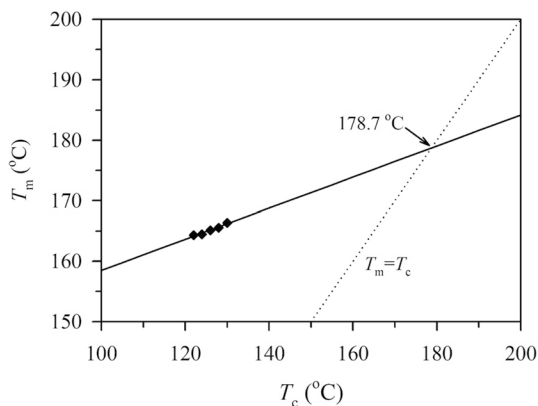
### Hoffman and Lauritzen theory

To perform the quantitative analysis of crystallization behavior and determine the temperature dependence of the crystallization rate, the equilibrium melting temperature ( $T_m^0$ ) must be determined. Hoffman–Weeks theory (Hoffman and Weeks 1962a; Hoffman 1983) stipulates that  $T_m^0$  is deduced by plotting the melting temperature ( $T_m$ ) against  $T_c$ . Figure 4 displays the plot of  $T_m$  versus  $T_c$ . The line of  $T_m = T_c$  was extrapolated.  $T_m^0$  was obtained by extrapolating the point of interest from the line of  $T_m = T_c$ , and the dependence of  $T_m$  on  $T_c$  is given by Eq. 2.

$$T_m = T_m^0(1 - \phi) + \phi T_c \quad (2)$$

where  $\phi$  ( $= 1/\gamma$ ) is the stability parameter, which is related to morphological factors concerning the perfectness and size of the crystal and  $\gamma$  is related to the final lamellar thickness, taken as the ratio of the lamellar thickness of a natural crystalline to the lamellar thickness of the critical crystalline nucleus.  $T_m^0$  and  $\phi$  values obtained are summarized in Table 2. The  $\phi$  value increased with increasing WPG from 0.26

**Fig. 4** Regression lines to equilibrium melting temperature proposed by Hoffman–Weeks extrapolation for polypropylene with unmodified bamboo fibers (WPG0)



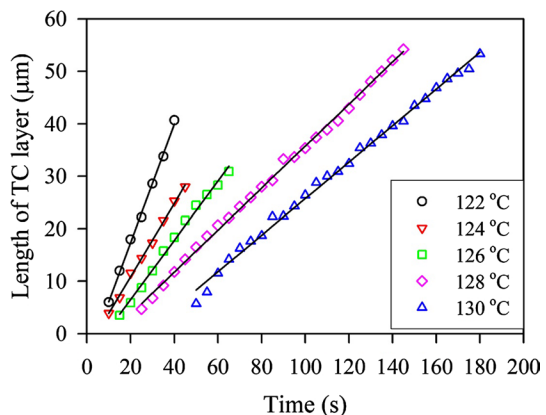


**Table 2** Equilibrium melting temperature ( $T_m^0$ ) and the stability parameter ( $\phi$ ) of polypropylene with various acetylated bamboo fibers (BFs) based on the Hoffman–Weeks extrapolation method

| BFs   | $T_m^0$ (°C) | $\phi$ | $R^2$ |
|-------|--------------|--------|-------|
| WPG0  | 178.7        | 0.26   | 0.961 |
| WPG2  | 187.4        | 0.37   | 0.953 |
| WPG6  | 185.7        | 0.36   | 0.949 |
| WPG9  | 190.9        | 0.40   | 0.954 |
| WPG19 | 192.0        | 0.42   | 0.994 |

(WPG0) to 0.42 (WPG19). A study (Hoffman and Weeks 1962b) reported that the  $\phi$  value is between 0 and 1, and a value below 0.4 suggests that crystals are reasonably stable. For a WPG of BF higher than 9%, the  $\phi$  value of acetylated BF/PP composites was higher than 0.4, indicating that these composites formed more unstable crystals. Moreover, the  $T_m^0$  value for WPG0 (178.7 °C) was the lowest among all the samples. When BF was acetylated, the  $T_m^0$  value of the BF/PP composite was higher than that of WPG0, and the value further increased from 187.4 °C for WPG2 to 192.0 °C for WPG19. Changes in the  $T_m^0$  value in BF/PP composites are caused by the different perfections and morphologies of the spherulite of the PP matrix (Bogoeva-Gaceva et al. 2001). These results suggest that the crystalline phase of the acetylated BF/PP composite is more perfect than that of the unmodified BF/PP composite. Figure 5 reveals the relationship between the length of the TC layer and crystallization time in unmodified BF/PP composites. The slope coefficients of lines represented the growth rates of the TC layer. As the crystallization temperature increases, the growth rate of the TC layer decreases. Similar results were observed in PP reinforced with different WPGs of acetylated BF (not shown). These results indicated that the length of the TC layer was strongly dependent on  $T_c$  and time.

To further investigate the crystallization behavior, the dependency of the crystal growth rate ( $G$ ) on  $T_c$  is expressed as follows, according to Hoffman–Lauritzen theory (Hoffman and Miller 1997):

**Fig. 5** Plots of the length of the TC layer against crystallization time for polypropylene with unmodified bamboo fibers (WPG0) surface under different crystallization temperatures

**Fig. 6** Hoffman–Lauritzen plots of polypropylene with various acetylated bamboo fibers

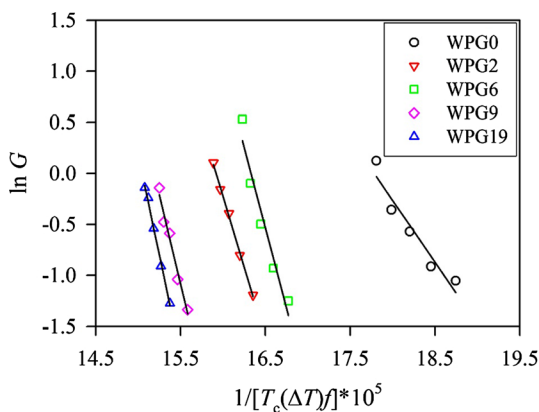


**Table 3** Fold surface interfacial free energies and work of chain folding for polypropylene with various acetylated bamboo fibers (BFs) based on Hoffman–Lauritzen theory

| BFs   | $K_g \times 10^{-5}$<br>(K <sup>2</sup> ) | $\sigma\sigma_c$<br>(erg <sup>2</sup> /cm <sup>4</sup> ) | $\sigma_c$<br>(erg/cm <sup>2</sup> ) | $q$<br>(kcal/mol) |
|-------|---|--|--------------------------------------|-------------------|
| WPG0  | 1.22                                      | 291.8  | 25.4                                 | 2.5               |
| WPG2  | 2.78                                      | 652.3  | 56.7                                 | 5.6               |
| WPG6  | 3.16                                      | 744.3  | 64.7                                 | 6.4               |
| WPG9  | 3.51                                      | 817.3  | 71.1                                 | 7.0               |
| WPG19 | 3.95                                      | 917.8  | 79.8                                 | 7.9               |

$$G = G_0 \exp\left(\frac{-U^*}{R(T_c - T_\infty)}\right) \exp\left(\frac{-K_g}{T_c(\Delta T)f}\right) \quad (3)$$

where  $G_0$  is a preexponential factor,  $U^*$  is an activation energy for segmental diffusion to the site of crystallization,  $R$  is the gas constant,  $T_\infty$  is the hypothetical temperature where all motion associated with viscous flow ceases,  $K_g$  is the nucleation parameter,  $\Delta T$  is the degree of supercooling defined by  $T_m^0 - T_c$ , and  $f$  is the correction factor defined as  $2T_c/(T_m^0 + T_c)$  that accounts for the change in heat of fusion with the crystallization temperature. Equation 3 can be converted into Eq. 4 by taking a natural logarithm of both sides:

$$\ln G + \frac{U^*}{R(T_c - T_\infty)} = \ln G_0 - \frac{K_g}{T_c(\Delta T)f} \quad (4)$$

Furthermore, Eq. 4 is simplified as follows:

$$\ln G = -\frac{K_g}{T_c(\Delta T)f} + \text{constant} \quad (5)$$

When plotting  $\ln G$  with  $1/[T_c(\Delta T)f]$  (Fig. 6), the value of  $K_g$  was obtained from the slope of a straight line.  $K_g$  values obtained from plots are listed in Table 3.

The  $K_g$  values of all acetylated BF/PP composites, which were in the range of  $2.78–3.95 \times 10^5 \text{ K}^2$ , were higher than the  $K_g$  values of unmodified BF/PP ( $1.22 \times 10^5 \text{ K}^2$ ). The  $K_g$  value of the acetylated BF/PP composite increased with increasing WPGs of acetylated BF. Furthermore, the folding-surface free energy ( $\sigma_e$ ) could be calculated from derived  $K_g$ . The nucleation parameter ( $K_g$ ) depends on the crystallization regime and the surface free energy and is defined as Eq. 6 (Hoffman 1983):

$$K_g = \frac{nb\sigma_e T_m^0}{k\Delta H_f^0} \quad (6)$$

where  $k$  is Boltzmann's constant ( $1.38 \times 10^{-16} \text{ erg/K}$ ),  $\Delta H_f^0$  is the heat of fusion of completely crystalline component per unit volume,  $\sigma$  is the lateral free energy of the growing crystal, and  $b$  is the thickness layer. Value  $n$  is a coefficient that depends on the crystallization regime and assigns the value 4 for regimes I and III and the value 2 for regime II. For the PP matrix,  $b$  is  $6.26 \times 10^{-8} \text{ cm}$ ,  $\Delta H_f^0$  is  $1.93 \times 10^9 \text{ erg/cm}^3$ , and  $\sigma$  is  $11.5 \text{ erg/cm}^2$  (Clark and Hoffman 1984). Furthermore, the mode of spherulite growth for PP is assumed to be regime III growth in this study; thus, its  $n$  value is theoretically given as 4. The subsequent results of the calculated folding-surface free energy ( $\sigma_e$ ) are summarized in Table 3. The  $\sigma_e$  values are 25.4, 56.7, 64.7, 71.1, and  $79.8 \text{ erg/cm}^2$  for WPG0, WPG2, WPG6, WPG9, and WPG19 of BF/PP composites, respectively. These results indicated that all acetylated BF/PP composites exhibited a higher  $\sigma_e$  value than did the unmodified BF/PP composite. To further investigate the bending of the polymer chain back upon itself, the work of chain folding ( $q$ ), which is strongly correlated with the  $\sigma_e$  value, was estimated using the following Eq. 7:

$$q = 2\sigma_e A_0 \quad (7)$$

where  $A_0$  is the cross-sectional area of the polymer matrix, and the value is  $34.4 \times 10^{-16} \text{ cm}^2$  (Clark and Hoffman 1984). The PP matrix with an unmodified BF (WPG0) had the lowest  $q$  value ( $2.5 \text{ kcal/mol}$ ) among all the samples. The value of the PP matrix with an acetylated BF increased with an increase in WPG. When BF was acetylated to 2% WPG, the  $q$  value increased to  $5.6 \text{ kcal/mol}$ . Furthermore, the  $q$  value significantly increased to  $7.9 \text{ kcal/mol}$  as WPG increased to 19%. The higher  $q$  value was principally caused by the presence of acetylated BF with higher WPG constraints on the mobility of PP matrix chains in interspherulitic regions. These findings not only further indicate that unmodified BF accelerates the crystallization of the PP matrix compared with acetylated BF, but also provide another explanation for why the crystallization rate of PP matrix with higher WPG acetylated BF is lower.

## Conclusion

In this study, the transcrystallization of the acetylated BF/PP composite under isothermal crystallization was investigated using various analytic techniques, such as POM and DSC. The formation and growth of the TC layer were strongly affected by the acetylation conditions of BFs. Hoffman–Lauritzen theory was used to calculate the folding-surface free energy ( $\sigma_e$ ) and the work of chain folding ( $q$ ) for each PP matrix with an unmodified or acetylated BF. The  $\sigma_e$  and  $q$  values of acetylated BF/PP composites obtained ranged from 56.7 to 79.8 erg/cm<sup>2</sup> and 5.6 to 7.9 kcal/mol, respectively. These values were higher than those for the unmodified BF/PP composite. These results support the notion that the presence of acetylated BF with a higher WPG significantly constrains the mobility of PP matrix chains in interspherulitic regions. Compared with unmodified BF, the addition of acetylated BF could affect the crystallization behavior of the PP matrix by inducing or hindering TC on the BF–PP interface. Therefore, these results provide useful information regarding manufacturing process conditions that could be used to optimize the polymer morphology in a composite.

**Acknowledgements** This work was financially supported by a research grant from the Forestry Bureau of the Council of Agriculture, Taiwan (109AS-10.8.1-FB-e2(2)).

## Declaration

**Conflicts of interest** The authors declare that there is no conflict of interest regarding the publication of this paper.

## References

- Bogoeva-Gaceva G, Janevski A, Mader E (2001) Nucleation activity of glass fibers towards iPP evaluated by DSC and polarizing light microscopy. *Polymer* 42:4409–4416. [https://doi.org/10.1016/S0032-3861\(00\)00659-5](https://doi.org/10.1016/S0032-3861(00)00659-5)
- Borysiak S (2013) Fundamental studies on lignocellulose/polypropylene composites: Effects of wood treatment on the transcrystalline morphology and mechanical properties. *J Appl Polym Sci* 102:804–809. <https://doi.org/10.1002/app.37651>
- Cai Y, Petermann J, Wittich H (1997) Transcrystallization in fiber-reinforced isotactic polypropylene composites in a temperature gradient. *J Appl Polym Sci* 65:67–75. [https://doi.org/10.1002/\(SICI\)1097-4628\(19970705\)65:1%3C67::AID-APP9%3E3.0.CO;2-O](https://doi.org/10.1002/(SICI)1097-4628(19970705)65:1%3C67::AID-APP9%3E3.0.CO;2-O)
- Chattopadhyay SK, Khandal RK, Uppaluri R, Ghoshal AK (2011) Bamboo fiber reinforced polypropylene composites and their mechanical, thermal, and morphological properties. *J Appl Polym Sci* 119:1619–1626. <https://doi.org/10.1002/app.32826>
- Chen X, Guo Q, Mi Y (1998) Bamboo fibre-reinforced polypropylene composite: a study of the mechanical properties. *J Appl Polym Sci* 69:1891–1899. [https://doi.org/10.1002/\(SICI\)1097-4628\(19980906\)69:10%3C1891::AID-APP1%3E3.0.CO;2-9](https://doi.org/10.1002/(SICI)1097-4628(19980906)69:10%3C1891::AID-APP1%3E3.0.CO;2-9)
- Cheng H, Gao J, Wang G, Shi SQ, Zhang S, Cai L (2015) Enhancement of mechanical properties of composites made of calcium carbonate modified bamboo fibers and polypropylene. *Holz-forschung* 69:215–221. <https://doi.org/10.1515/hf-2014-0020>
- Clark EJ, Hoffman JD (1984) Regime III crystallization in Polypropylene. *Macromolecules* 17:878–885. <https://doi.org/10.1021/ma00134a058>

- Das M, Chakraborty D (2008) Evaluation of improvement of physical and mechanical properties of bamboo fibres due to alkali treatment. *J Appl Polym Sci* 107:522–527. <https://doi.org/10.1002/app.26155>
- Deshpande AP, Bhaskar Rao M, Laksjmana Rao C (2000) Extraction of bamboo fibers and their use as reinforcement in polymeric composites. *J Appl Polym Sci* 76:83–92. [https://doi.org/10.1002/\(SICI\)1097-4628\(20000404\)76:1%3C83::AID-APP11%3E3.0.CO;2-L](https://doi.org/10.1002/(SICI)1097-4628(20000404)76:1%3C83::AID-APP11%3E3.0.CO;2-L)
- Gao Y, Wu Y, Liang M, Fu Q (2015) Transcrystallinity and relevant interfacial strength induced by carbon nanotube fibers in a polypropylene matrix. *J Appl Polym Sci* 132:42119–42124. <https://doi.org/10.1002/app.42119>
- Han S, Ren K, Geng C, Wang K, Zhang Q, Chen F, Fu Q (2014) Enhanced interfacial adhesion via interfacial crystallization between sisal fiber and isotactic polypropylene: direct evidence from single-fiber fragmentation testing. *Polym Int* 63:646–651. <https://doi.org/10.1002/pi.4551>
- Hoffman JD (1983) Regime III crystallization in melt-crystallized polymers: The variable cluster model of chain folding. *Polymer* 24:3–26. [https://doi.org/10.1016/0032-3861\(83\)90074-5](https://doi.org/10.1016/0032-3861(83)90074-5)
- Hoffman JD, Miller RL (1997) Kinetics and crystallization from the melt and chain folding in polyethylene fractions revisited: theory and experiment. *Polymer* 38:3151–3212. [https://doi.org/10.1016/S0032-3861\(97\)00071-2](https://doi.org/10.1016/S0032-3861(97)00071-2)
- Hoffman JD, Weeks JJ (1962a) Melting process and the equilibrium melting temperature of polychlorotrifluoroethylene. *J Res Natl Bur Stand Sect A* 66:13–28
- Hoffman JD, Weeks JJ (1962b) Rate of spherulitic crystallization with chain folds in polychlorotrifluoroethylene. *J Chem Phys* 37:1723–1741. <https://doi.org/10.1063/1.1733363>
- Hsu C-Y, Yang T-C, Wu T-L, Hung K-C, Wu J-H (2018) The influence of bamboo fiber content on the non-isothermal crystallization kinetics of bamboo fiber-reinforced polypropylene composites (BPCs). *Holzforschung* 72:329–336. <https://doi.org/10.1515/hf-2017-0046>
- Hung K-C, Wu J-H (2010) Mechanical and interfacial properties of plastic composite panels made from esterified bamboo particles. *J Wood Sci* 56:216–221. <https://doi.org/10.1007/s10086-009-1090-9>
- Hung K-C, Chen Y-L, Wu J-H (2012) Natural weathering properties of acetylated bamboo plastic composites. *Polym Degrad Stab* 97:1680–1685. <https://doi.org/10.1016/j.polymdegradstab.2012.06.016>
- Hung K-C, Wu T-L, Chen Y-L, Wu J-H (2016) Assessing the effect of wood acetylation on mechanical properties and extended creep behavior of wood/recycled-polypropylene composites. *Constr Build Mater* 108:139–145. <https://doi.org/10.1016/j.conbuildmat.2016.01.039>
- Ismail H, Edyham MR, Wirjosentono B (2002) Bamboo fibre filled natural rubber composites: the effects of filler loading and bonding agent. *Polym Test* 21:139–144. [https://doi.org/10.1016/S0142-9418\(01\)00060-5](https://doi.org/10.1016/S0142-9418(01)00060-5)
- Jhu Y-S, Yang T-C, Hung K-C, Xu J-W, Wu T-L, Wu J-H (2019) Nonisothermal crystallization kinetics of acetylated bamboo fiber-reinforced polypropylene composites. *Polymers* 11:1078. <https://doi.org/10.3390/polym11061078>
- Kamal MR, Chu E (1983) Isothermal and nonisothermal crystallization of polyethylene. *Polym Eng Sci* 23:27–31. <https://doi.org/10.1002/pen.760230107>
- Keener TJ, Stuart RK, Brown TK (2004) Maleated coupling agents for natural fibre composites. *Compos Part A-Appl S* 35:357–362. <https://doi.org/10.1016/j.compositesa.2003.09.014>
- Li Y, Yin L, Huang C, Meng Y, Fu F, Wang S, Wu Q (2015) Quasi-static and dynamic nanoindentation to determine the influence of thermal treatment on the mechanical properties of bamboo cell walls. *Holzforschung* 69:909–914. <https://doi.org/10.1515/hf-2014-0112>
- Lisperguer J, Droguett C, Ruf B, Nunez M (2007) The effect of wood acetylation on thermal behavior of wood-polystyrene composites. *J Chilean Chem Soc* 52:1073–1075. <https://doi.org/10.4067/S0717-97072007000100004>
- Liu H, Jiang Z, Fei B, Hse C, Sun Z (2015) Tensile behaviour and fracture mechanism of moso bamboo (*Phyllostachys pubescens*). *Holzforschung* 69:47–52. <https://doi.org/10.1515/hf-2013-0220>
- Liu Z, Fei B, Jiang Z, Cai Z, Liu X (2014) Important properties of bamboo pellets to be used as commercial solid fuel in China. *Wood Sci Technol* 48:903–917. <https://doi.org/10.1007/s00226-014-0648-x>
- Liu H, Wang X, Zhang X, Sun Z, Jiang Z (2016) In situ detection of the fracture behaviour of moso bamboo (*Phyllostachys pubescens*) by scanning electron microscopy. *Holzforschung* 70:1183–1190. <https://doi.org/10.1515/hf-2016-0003>
- Mori Y, Kuwano Y, Tomokiyo S, Kuroyanagi N, Odahara K (2019) Inhibitory effects of Moso bamboo (*Phyllostachys heterocycla f. pubescens*) extracts on phytopathogenic bacterial and fungal growth. *Wood Sci Technol* 53:135–150. <https://doi.org/10.1007/s00226-018-1063-5>

- Okubo K, Fujii T, Yamamoto Y (2004) Development of bamboobased polymer composites and their mechanical properties. *Compos Part A-Appl S* 35:377–383. <https://doi.org/10.1016/j.compositesa.2003.09.017>
- Phuong NT, Girbert V (2010) Non-isothermal crystallization kinetics of short bamboo fiber-reinforced recycled polypropylene composites. *J Reinf Plast Compos* 28:1–16. <https://doi.org/10.1177/0731684409355604>
- Quan H, Lin Z-M, Yang M-B, Huang R (2005) On transcrystallinity in semi-crystalline polymer composites. *Compos Sci Technol* 65:999–1021. <https://doi.org/10.1016/j.compotech.2004.11.015>
- Rowell RM (1983) Chemical modification of wood. *For Prod Abstr* 6:363–382
- Scurlock JMO, Dayton DC, Hames B (2000) Bamboo: an overlooked biomass resource? *Biomass Bioenerg* 19:229–244. [https://doi.org/10.1016/S0961-9534\(00\)00038-6](https://doi.org/10.1016/S0961-9534(00)00038-6)
- Supaphol P, Spruiell JE (2001) Isothermal melt- and cold-crystallization kinetics and subsequent melting behavior in syndiotactic polypropylene: a differential scanning calorimetry study. *Polymer* 42:699–712. [https://doi.org/10.1016/S0032-3861\(00\)00399-2](https://doi.org/10.1016/S0032-3861(00)00399-2)
- Thomason JL, Van Rooyen AA (1992) Transcrystallized interphase in thermoplastic composites. *J Mater Sci* 27:889–896. <https://doi.org/10.1007/BF01197639>
- Wang C, Liu C-R (1999) Transcrystallization of polypropylene composites: nucleating ability of fibers. *Polymer* 40:289–298. [https://doi.org/10.1016/S0032-3861\(98\)00240-7](https://doi.org/10.1016/S0032-3861(98)00240-7)
- Wang Y, Weng Y, Wang L (2014) Characterization of interfacial compatibility of polylactic acid and bamboo flour (PLA/BF) in biocomposites. *Polym Test* 36:119–125. <https://doi.org/10.1016/j.polymertesting.2014.04.001>
- Yang T-C, Wu T-L, Hung K-C, Chen Y-L, Wu J-H (2015) Mechanical properties and extended creep behavior of bamboo fiber reinforced recycled poly(lactic acid) composites using the time-temperature superposition principle. *Constr Build Mater* 93:558–563. <https://doi.org/10.1016/j.conbuildmat.2015.06.038>

**Publisher's Note** Springer Nature remains neutral with regard to jurisdictional claims in published maps and institutional affiliations.